Received: 24 March 2023 | Revised: 20 July 2023 | Accepted: 16 August 2023

DOI: 10.1111/pce.14704

ORIGINAL ARTICLE

Plant, Cell & Environment | WILEY

Wood-density has no effect on stomatal control of leaf-level water use efficiency in an Amazonian forest

Julien Lamour[1,2] | Daisy C. Souza[3] | Bruno O. Gimenez[3,4] | Niro Higuchi[3] | Jérôme Chave[2] | Jeffrey Chambers[4] | Alistair Rogers[1]

[1]Department of Environmental & Climate Sciences, Brookhaven National Laboratory, Upton, New York, USA

[2]Evolution and Biological Diversity (EDB), CNRS/IRD/UPS, Toulouse, France

[3]National Institute of Amazonian Research (INPA), Forest Management Laboratory (LMF), Manaus, Amazonas, Brazil

[4]Department of Geography, University of California, Berkeley, California, USA

Correspondence

Julien Lamour and Alistair Rogers, Department of Environmental and Climate Sciences, Brookhaven National Laboratory, Upton, NY, USA.
Email: jlamour.sci@gmail.com and arogers@bnl.gov

Funding information

United States Department of Energy, Grant/Award Number: DE-SC0012704

Abstract

Forest disturbances increase the proportion of fast-growing tree species compared to slow-growing ones. To understand their relative capacity for carbon uptake and their vulnerability to climate change, and to represent those differences in Earth system models, it is necessary to characterise the physiological differences in their leaf-level control of water use efficiency and carbon assimilation. We used wood density as a proxy for the fast-slow growth spectrum and tested the assumption that trees with a low wood density (LWD) have a lower water-use efficiency than trees with a high wood density (HWD). We selected 5 LWD tree species and 5 HWD tree species growing in the same location in an Amazonian tropical forest and measured in situ steady-state gas exchange on top-of-canopy leaves with parallel sampling and measurement of leaf mass area and leaf nitrogen content. We found that LWD species invested more nitrogen in photosynthetic capacity than HWD species, had higher photosynthetic rates and higher stomatal conductance. However, contrary to expectations, we showed that the stomatal control of the balance between transpiration and carbon assimilation was similar in LWD and HWD species and that they had the same dark respiration rates.

KEYWORDS

climax, leaf traits, photosynthesis, pioneer, stomatal conductance, succession, terrestrial biosphere models

1 | INTRODUCTION

Stomata play a major role in the regulation of global CO_2 and water vapour fluxes, balancing the processes of photosynthesis and transpiration, which account for ~55% of global carbon dioxide uptake and >80% of terrestrial evapotranspiration, respectively (Friedlingstein et al., 2022; Jasechko et al., 2013). Accurate representation of stomatal control in Earth system models (ESMs) is therefore central to improved prediction of these fluxes, particularly in tropical forests, which cycle more CO_2 and water than any other biome (Beer et al., 2010; Schlesinger & Jasechko, 2014).

Understanding how tropical forests will be affected by climate change requires representation of species diversity, including differences in their capacity for CO_2 assimilation and stomatal control of water loss that drive their response to hotter, drier air, and their vulnerability to drought (Oliveira et al., 2021; Poorter et al., 2019; Rogers et al., 2017). ESMs account for species diversity by grouping plants with similar structural and functional properties into groups called plant functional types (PFTs). Currently, ESMs represent tropical forests using only one or two PFTs, hampering the representation of shifts in ecosystem composition that may affect the carbon and water cycles (Fisher et al., 2014, 2018; Franklin et al., 2020; Poulter et al., 2011). Of particular importance is the need to better represent the ecological succession of species (Nyirambangutse et al., 2017; Reich, 2014; Rüger et al., 2020; Swaine & Whitmore, 1988) to enable a more realistic representation of

ecosystem response to disturbance. Early successional species are the first ones to grow after the opening of a gap, other disturbance, or deforestation (Bazzaz & Pickett, 1980; Shugart, 1984). In wet tropical forests, they have a low wood density (LWD), are fast-growing, light-demanding, have high maximum rates of photosynthesis and relatively short-lived leaves (Chave et al., 2009; Poorter et al., 2019; Swaine & Whitmore, 1988; Wright et al., 2004). They differ from late successional species that survive for prolonged periods of time, slowly growing in the shady understory after the forest canopy closes. These late successional species typically have a higher wood density, lower maximum photosynthetic rates and relatively long-lived leaves (Bazzaz & Pickett, 1980; Reich et al., 1991, 1995). Early successional species represent an increasing proportion of the total species found in tropical forests (Jakovac et al., 2022). This is due to an increase in disturbance in old-growth forests that leads to colonisation by early successional species (Asner et al., 2005; Gaui et al., 2019; Ordway & Asner, 2020; Rangel Pinagé et al., 2019) and an increase in the proportion of secondary-growth forests of less than 60 years (Chazdon et al., 2016; Poorter et al., 2016). It has been shown that early successional species can markedly impact the carbon cycle and represent a strong sink for atmospheric CO_2 (Chazdon et al., 2016; Rangel Pinagé et al., 2022; but see Mills et al., 2023). However, current ESMs do not represent this variation, preventing accurate prediction of the vulnerability of this important biome to climate change.

In this study, we focused our measurements on understanding potential differences in the leaf-level water-use efficiency (WUE) in early and late successional species to determine if separate parameterisation for stomatal control would be required to represent fast and slow-growing PFTs in ESMs. Leaf-level WUE is the amount of carbon assimilated per unit of water vapour lost through transpiration (Bonan et al., 2014; Medlyn et al., 2011). It is determined by the leaf capacity for CO_2 assimilation and by the stomatal control of CO_2 and water vapour diffusion. Leaf-level WUE of early and late successional tropical species has been studied using various approaches. This includes the gas exchange measurement of the ratio of light-saturated photosynthesis to stomatal conductance (A_{sat}/g_{sw}) or transpiration (A_{sat}/E), and measurement of leaf carbon isotope discrimination. These approaches led to contrasting results, with either a higher leaf-level-WUE in late successional species (Huc et al., 1994), no effect (Apgaua et al., 2017; Bonal et al., 2007), or lower WUE (Nogueira et al., 2004). Interpreting the contrasting results obtained in these studies is difficult as the metrics of WUE differed (A_{sat}/g_{sw}, A_{sat}/E, and isotope discrimination) and are known to vary with environmental variables (Medlyn et al., 2011, 2017). In addition, A_{sat}, g_{sw}, and E are usually outputs of the gas exchange equations used in ESMs so these metrics can't be used to parameterise ESMs that rely instead on traits associated with stomatal conductance and photosynthesis (Rogers et al., 2017).

In this study, we examined the stomatal control of CO_2 and water vapour diffusion using the unified stomatal optimisation model (USO; Medlyn et al., 2011, Equation 1), which has been implemented in several ESMs (De Kauwe et al., 2015; Franks et al., 2018; Li et al., 2022; Oliver et al., 2018). The USO model is interpretable within the optimal theory presented by Cowan & Farquhar (1977), where stomatal conductance to water vapour (g_{sw}) reacts to changes in the environment such as light, CO_2, and leaf-to-air vapour pressure deficit (VPD_{leaf}) to maximise CO_2 assimilation (A) for a given water supply (Buckley et al., 2017). In this model, the stomatal slope parameter (g_1) is a constant that is inversely proportional to the leaf-level WUE defined as the marginal carbon gain of transpiration water loss (WUE = $\frac{\partial A}{\partial E}$, Bonan et al., 2014; Medlyn et al., 2011). It has been shown that g_1 vary with species, environment, and season (Lin et al., 2015; Miner et al., 2017; Wolz et al., 2017; Zhou et al., 2013) and can drive a large degree of uncertainty in many model outputs (Dietze et al., 2014; Knauer et al., 2015; Migliavacca et al., 2021; Ricciuto et al., 2018) further motivating the need to better characterise this parameter in tropical forest species. Another key parameter in the USO model is g_0 which represents the stomatal conductance when A is zero. This parameter is not predicted by optimality (Cowan & Farquhar, 1977) and was included in the USO model to account for empirical evidence that g_{sw} is always positive due to cuticular conductance and leaky stomata (Duursma et al., 2019).

$$g_{sw} = g_0 + 1.6\left(1 + \frac{g_1}{\sqrt{VPD_{leaf}}}\right)\frac{A}{CO_2}. \quad (1)$$

Because the g_1 parameter is interpretable in the optimality framework (Cowan & Farquhar, 1977); Héroult et al. (2013) and Lin et al. (2015) developed hypothesis for how it should vary with environmental conditions and other plant traits. They predicted that g_1 should be inversely related to wood density due to the higher cost of wood construction per unit of water transported. Therefore, early successional species are expected to have a higher g_1 (lower leaf-level WUE) than late successional species. In their synthesis, Lin et al. (2015) found a negative relationship between g_1 and wood density across plants from different biomes providing empirical support for this theoretical relationship. Héroult et al. (2013) also found a negative relationship between g_1 and wood density in *Eucalyptus* species from contrasting climates. If this theory is broadly supported by empirical data, it could be incorporated into ESMs to define new PFTs along the slow-fast growth continuum. However, it remains to be seen if this relationship holds in tropical forests and, importantly, if the relationship can be observed in trees measured in the same environmental conditions. In addition, Lamour et al. (2022a) observed that the g_1 parameter in Medlyn et al.s' (2011) USO model was not a constant for a leaf but varied with the photosynthetic rate, and they suggested that the comparison of leaf-level WUE of species with contrasting photosynthetic capacities could potentially confound interpretation.

In this study, we provide a direct evaluation of the hypothesis presented by Lin et al. (2015) that g_1 is negatively correlated with wood density—that is, that early successional, low wood density (LWD) species have a lower leaf-level WUE than late successional, high wood density (HWD) species—in an Amazonian wet tropical

forest. Importantly we aimed to evaluate this hypothesis in co-occurring species where the soil type, local hydrology, climate and weather would not confound analysis. Following the hypothesis presented by Lin et al. (2015), we used the USO model to estimate g_1 and evaluate its relationship with wood density. We also used the Lamour et al. (2022a) conductance model (Lamour model, hereafter) to evaluate if potential differences in leaf-level WUE efficiency could be explained by variation in photosynthetic capacity. Furthermore, measurements were made on intact branches where care was taken to ensure that stomatal conductance fully acclimated to the measurement conditions. This approach was taken to avoid any possible bias associated with the slow response of stomata or with the excision of branches (Davidson et al., 2023; Miner et al., 2017; Wolz et al., 2017).

2 | MATERIAL AND METHODS

2.1 | Field site

The study was carried out in the Biomass and Nutrient Experiment (BIONTE) site at the Experimental Station of Tropical Forestry (E.E.S.T—ZF-2, 2° 38′ 17″S, 60° 09′ 25″W) managed by the National Institute for Amazon Research (INPA) and located approximately 60 km NW of Manaus, Brazil. The climate of the site (Figure 1) is characterised as Af (tropical) according to Köppen's system, with 2250 mm average annual rainfall and with a mean annual temperature around 27°C (Meng et al., 2022; Spanner et al., 2022). The site is located in a plateau area located above the Amazon flood plains (*terra firme*) and classified as well-drained high clay content dystrophic yellow latosol (DeArmond et al., 2019). The area is populated by an old-growth forest which, as part of the BIONTE experiment, was disturbed by selective logging in the mid-1980s. All the trees above 55 cm in diameter were removed to study the effect on growth, competition, mortality and recruitment (Amaral et al., 2019; Higuchi et al., 1997). The selective logging created gaps among the older trees in which early successional species grew. As a result, this manipulation enabled us to sample early and late successional species in the same location, which limited the potential confounding effect of soil variation if early and late successional species were sampled in different sites. A trail was built for selective logging in the 1980s and subsequently maintained enabling access to the trees used in this study.

2.2 | Canopy tree species sampling

We choose 10 species with contrasting wood density ($n = 5$ LWD trees and $n = 5$ HWD trees, Table 1) from the global wood density database (Chave et al., 2009; Zanne et al., 2009). The five low-density species had a wood density below 0.49 g cm^{-3} (dry mass per unit of fresh volume, Table 1). They include common pioneer species (*Cecropia sciadophylla* Mart., *Pourouma guianensis* Aubl., *Pourouma velutina* Mart. Ex Miq., *Vismia guianensis* (Aubl.) Pers.) and *Ocotea floribunda* (Sw.) Mez, which also has a LWD but is not commonly found in secondary forests. The five HWD species had a density above 0.75 g cm^{-3}. They include typical old-growth Amazon forest species (*Lecythis prancei* S.A. Mori, *Eschweilera atropetiolata* S.A. Mori, *Swartzia arborescens* (Aubl.) Pittier, *Inga paraensis* Ducke, and *Geissospermum argenteum* Woodson). Measurements were made on top-of-canopy, fully-expanded, and physiologically mature sun

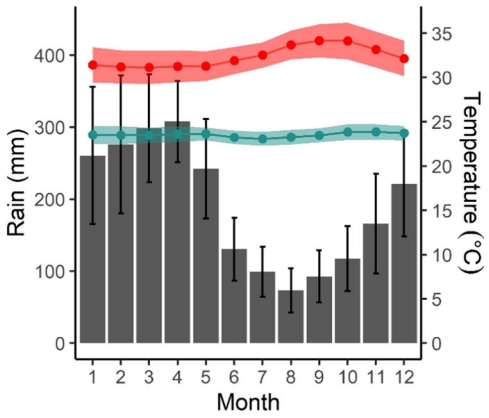

FIGURE 1 Average meteorological conditions for the study site. Data was sourced from a weather station situated 50 km from the site that has been in operation since the 1980s (Meng et al., 2022). The bars represent the monthly average precipitation, the lines represent the average minimum (blue) and maximum (red) monthly air temperature. The error bars and the shaded area represent the standard deviation of the monthly average.

TABLE 1 Description of the trees.

Species	Height	DBH	WD
Cecropia sciadophylla Mart.	23.7	22.1	0.32
Eschweilera atropetiolata S.A. Mori	20.3	19.9	0.75
Geissospermum argenteum Woodson	23	77.6	0.85
Inga paraensis Ducke	24.3	26.7	0.82
Lecythis prancei S.A. Mori	29	56.1	0.75
Ocotea floribunda (Sw.) Mez	19.8	15.1	0.46
Pourouma guianensis Aubl.	23.5	33	0.36
Pourouma velutina Mart. ex Miq.	22.9	27.1	0.28
Swartzia arborescens (Aubl.) Pittier	22	27.7	0.78
Vismia guianensis (Aubl.) Pers.	13.2	14.9	0.49

Note: The height in metres of the tree was measured at the top-of-canopy with a weighted tape. DBH corresponds to the diameter at breast height (cm), and the wood density (WD) corresponds to the average value for the species or the genus obtained from a global wood density database (Chave et al., 2009; Zanne et al., 2009), with more recent updates. Names and authorities are after the World Flora Online (http://www.worldfloraonline.org/).

exposed leaves. Leaves were accessed using a four-wheel-drive articulated boom lift (model Genie Z80/60) that can extend to a maximum vertical height of 26 m. The study was carried out in August and early September 2022 during the dry season (Figure 1).

2.3 | Gas exchange measurements

Gas exchange measurements were made with a LI-6400XT gas exchange system (LI-COR) with a $2 \times 3\,cm^2$ leaf chamber, equipped with an advanced polymer gasket and a red/blue light source (6400-02B LED light source; LI-COR) set to a 90% red, 10% blue ratio. The LI-6400XT power was supplied by an external battery (Super High Capacity Rechargeable Battery) or directly by the lift power, which was accessible from the platform. Measurements were conducted from 7 AM to 6 PM and followed the classic survey-type approach (Bernacchi et al., 2006; Wu et al., 2020), where the LI-6400XT conditions are controlled and set to match ambient conditions measured adjacent to the leaf immediately before measurement. The incident irradiance was measured with the external quantum sensor of the LI-6400XT. The block temperature of the LI-6400XT was set to the ambient temperature measured with a handheld weather station that can measure air temperature, relative humidity and wind speed (Kestrel 5500 Weather Meter, Nielsen-Kellerman Co.). The humidity was not modified by the LI-6400XT instrument (desiccant on full bypass). The reference CO_2 concentration was set to 410 ppm and the flow rate to 500 µmol s^{-1}. Before clamping the leaf, we started the auto-logging programme of the LI-6400XT and recorded gas exchange measurements every 5 s. After a minimum of 20 min, we assessed stability of leaf gas exchange. If the photosynthetic rate (A) and the leaf stomatal conductance to water vapour (g_{sw}) were not stable, that is, showed a visible downward or upward trend over the preceding 4 min, we continued collecting data until steady-state gas exchange was observed (always within 32 min).

In addition to these survey-type measurements where the irradiance was set to the ambient irradiance, we also conducted measurements at a predetermined setpoint of 100 µmol m^{-2} s^{-1} and at a saturating irradiance of 1800 µmol m^{-2} s^{-1}. These measurements were added to ensure that we had a wide and comparable range of measurements for all the species and included measurement of the light-saturated photosynthetic rate (A_{sat}), the conductance at saturating light ($g_{sw,sat}$) and to enable the calculation of the maximum carboxylation capacity of Rubisco (V_{cmax}) using the one-point method (Burnett et al., 2019; De Kauwe et al., 2016).

We also conducted dark-adapted leaf gas exchange measurements. We used the LI-6400XT as described previously with the light source off and the flow rate reduced to 300 µmol s^{-1}. We covered the leaf and the LI-6400XT head with a dark cloth and waited for the stability of A and g_{sw}. The dark-adapted A value corresponded to the dark respiration rate (R_{dark}) and the dark-adapted value of g_{sw} to $g_{sw,dark}$. These measurements were conducted in the late afternoon as $g_{sw,dark}$ took too long to stabilise in the morning. For each species gas exchange measurements were made on different leaves of the same tree ($n = 6–9$ per species).

2.4 | Estimation of the dark respiration and maximum carboxylation capacity at 25°C

We scaled the dark respiration, R_{dark}, to 25°C (R_{dark25}) using an Arrhenius function parametrised with the activation parameter from Bernacchi et al. (2001). We estimated the maximum carboxylation capacity, $V_{cmax,}$ using the "one-point method" (De Kauwe et al., 2016). The calculation uses the measurement of steady-state A_{sat}, the corresponding intracellular CO_2 concentration and an estimate of the leaf respiration, which is commonly assumed to be 1.5% of V_{cmax}. To reduce uncertainty in V_{cmax} estimated using the one-point approach, we used the species averaged R_{dark25} that we scaled to the measurement leaf temperature. This was done because we observed that although the A_{sat} was markedly different between LWD and HWD species, the R_{dark} was the same, suggesting that a different ratio should be considered for both species in place of the fixed ratio of 1.5%. We scaled V_{cmax} estimated at leaf temperature to the reference temperature of 25°C (V_{cmax25}) using a modified Arrhenius function (Leuning, 2002) parametrised with the activation parameters described by Bernacchi et al. (2001) and the deactivation parameters from Leuning (2002) as is commonly done in ESMs (Bonan et al., 2011; Oleson et al., 2013).

2.5 | Leaf conductance traits

We estimated g_1 and g_0 of the USO model (Medlyn et al., 2011, Equation 1). We also used the Lamour et al. (2022a) model (Lamour model, Equation 2).

$$g_{sw} = g_0 + c_{g1}\frac{1.6(A + R_{dark})^2}{\sqrt{VPD_{leaf}}CO_2}. \quad (2)$$

This model is based upon the USO model but was modified to account for the empirical evidence that g_{sw} varies non-linearly with the photosynthesis rate. The USO equation assumes that g_1 is independent of A whereas the Lamour model (Equation 2) implies that g_1 of the USO model increases proportionally to the net photosynthesis rate with a coefficient c_{g1}, and therefore that leaves are less water-use-efficient at high A. In the Lamour model, g_0 corresponds to the conductance in the dark ($g_{sw,dark}$), whereas in the USO model g_0 corresponds to the conductance at the light compensation point. For both models, we used the CO_2 concentration measured in the leaf chamber, which is more representative of the CO_2 concentration at the leaf surface than the reference CO_2.

2.6 | Leaf mass per surface area and nitrogen content of the leaves

Following gas exchange measurements, we collected between 5 and 10 leaf discs of known area. These were dried to constant mass at 60°C. We then measured their mass and calculated the leaf dry mass

per unit surface area (LMA g leaf area g^{-1} dry mass). These samples (c. 5 per tree) were subsequently ground before analysis for elemental composition to determine N content on a mass basis (N_m mg N g^{-1} dry mass). Samples were analysed using a 2400 Series II CHNS/O Elemental Analysis (PerkinElmer) following manufacturer instructions. The N content was then expressed on a surface area basis (N_{area} g N m^{-2} leaf area) using LMA.

We calculated the fraction of leaf nitrogen invested in Rubisco (F_{LNR} in %) following Equation (3) (Rogers, 2014; Thornton & Zimmermann, 2007), where F_{NR} is the mass ratio of total Rubisco molecular mass to nitrogen in Rubisco and a_{R25} is the specific activity of rubisco at 25°C.

$$F_{LNR} = \frac{V_{cmax25}}{N_a F_{NR} a_{R25}}. \quad (3)$$

F_{NR} and a_{R25} are constants that we set to 6.22 g Rubisco g^{-1} N in Rubisco and 47.3 µmol CO_2 g^{-1} Rubisco s^{-1}, respectively, following Rogers (2014). Note that these calculations assume an infinite mesophyll conductance such that the CO_2 concentration at the active site of Rubisco is considered equal to C_i. This assumption is consistent with the approach adopted by most ESMs.

2.7 | Species diameter growth rate

We calculated the diameter growth rate of the species that we selected for gas exchange measurements using the site forest inventory database (Higuchi et al., 1997), which includes the diameter at breast height (DBH) of all the trees above 10 cm measured yearly since 1980. We selected all the individuals included in the census, removed clear DBH outliers manually (typing errors) and calculated the average growth rate for each tree using a linear regression between the DBH and the year, where the tree average growth rate corresponded to the slope of the regression. The inventory database contained $n = 2$–24 individuals of each species. *V. guianensis* and *S. arborescens* were the less represented ($n = 2$ and $n = 4$ trees, respectively). At least $n = 9$ individuals were measured for the other species. The tree growth rates were used to estimate the relationship between the average species wood density (Table 1) and their average growth rate (see Section 2.8).

2.8 | Statistical analysis

To estimate the effect of waiting for the stability of A and g_{sw} on the estimation of g_1 and c_{g1}, we averaged 20 s of gas exchange measurements centred 90 s after clamping on the leaf and at steady-state. We used the 20-s-average of A, g_{sw}, CO_2, and VPD_{leaf} to estimate g_1 and c_{g1} of the USO and Lamour models using Equations (4) and (5), respectively (Hasper et al., 2017).

$$g_1 = \frac{g_{sw} - g_0 - \frac{1.6A}{CO_2}}{\frac{1.6A}{\sqrt{VPD_{leaf}}\,CO_2}}, \quad (4)$$

$$c_{g1} = \frac{g_{sw} - g_0}{\frac{1.6(A + R_{dark})^2}{\sqrt{VPD_{leaf}}\,CO_2}}. \quad (5)$$

The estimation of g_1 and c_{g1} with these equations requires an estimate of g_0 which we assumed to be constant at the average $g_{sw,\,dark}$ we measured in this study (0.01 mol m^{-2} s^{-1}). Equation (5) also requires an estimate of R_{dark}. We considered that R_{dark} corresponded to the mean value of R_{dark25} scaled to the measured leaf temperature using an Arrhenius function as described previously. Finally, we compared g_1 and c_{g1} estimated at 90 s, a typical time at which survey measurements are taken (Davidson et al., 2023; Wu et al., 2020) and at steady-state using a paired t-test. All the other analyses presented here use the gas exchange values taken at steady state.

To estimate the effect of the wood density on the parameters g_0 and g_1 we first reformulated the USO and Lamour model as linear models, using changes of variables (Equation 6, Table 2). In this form g_0 is the intercept of the model and m is the slope which corresponds to g_1 for the USO model and to c_{g1} for the Lamour Model (Davidson et al., 2022; Lamour et al., 2022a).

$$Y = g_0 + mX. \quad (6)$$

TABLE 2 The USO (row 1) and Lamour (row 2) conductance models rearranged in the linear form $Y = g_0 + mX$ where g_0 is the intercept, m is the conductance slope, and X is the regressor.

Y	m	X	$g_{sw,dark}$	Predicted g_{sw}
$g_{sw} - \frac{1.6A}{CO_2}$	g_1	$\frac{1.6A}{\sqrt{VPD_{leaf}}\,CO_2}$	$g_0 - 1.6\left(1 + \frac{g_1}{\sqrt{VPD_{leaf}}}\right)\frac{R_{dark}}{CO_2}$	$g_0 + 1.6\left(1 + \frac{g_1}{\sqrt{VPD_{leaf}}}\right)\frac{A}{CO_2}$
g_{sw}	c_{g1}	$\frac{1.6(A + R_{dark})^2}{\sqrt{VPD_{leaf}}\,CO_2}$	g_0	$g_0 + c_{g1}\frac{1.6(A + R_{dark})^2}{CO_2}$

Note: g_0 and $g_{sw,dark}$ are expressed in mol m^{-2} s^{-1}, g_1 in kPa0.5 and c_{g1} in µmol^{-1} m^2 s kPa0.5. g_0 has a different mathematical value in the unified stomatal optimization (USO) and Lamour models as a result of having A or $A + R_{dark}$ in the denominator of X. The value of the conductance in the dark ($g_{sw,dark}$) in function to g_0 is given in the column $g_{sw,dark}$.

We then studied the effect of wood density using a mixed model (Equation 7) where the species has a random effect on the intercept (g_0) and the slope (m) of the regression.

$$Y = g_0 + a + \alpha + (m + b + \beta)X + \varepsilon. \quad (7)$$

In Equation (7), a and b are the fixed effect of the wood density class (High or Low) on g_0 and m, respectively; α and β are the random effect of the species on g_0 and m, respectively, $\alpha \sim N(0, \sigma_\alpha^2)$, and $\beta \sim N(0, \sigma_\beta^2)$, and ε is the residual of the model, $\varepsilon \sim N(0, \sigma^2)$.

We estimated the parameters of Equation (7) using either all the steady-state gas exchange measurements or a subset of the measurements where we only kept the measurements made at an irradiance below 500 µmol m^{-2} s^{-1}. We used this subset because the USO model was derived mathematically by assuming that the stomata optimise the electron-transport limited photosynthetic rate (light limited photosynthesis, Medlyn et al., 2011). Note that further work showed that this assumption could bias the estimation of g_1 when the photosynthesis is limited by the rate of Rubisco carboxylation, a limitation which typically occurs at high irradiance (Buckley et al., 2017; Dewar et al., 2018; Huang et al., 2021; Lamour et al., 2022a; Prentice et al., 2014). We chose the conservative value of 500 µmol m^{-2} s^{-1} to be sure to avoid light saturated photosynthesis rates.

We assessed the performance of the USO and Lamour models by comparing the Akaike Information Criterion of information (Akaike, 1974) and σ (Equation 7).

We estimated the effect of the wood density classes on $g_{sw,dark}$, $g_{sw,sat}$, R_{dark25}, V_{cmax25}, LMA, N_{area}, and F_{LNR} by using a mixed model with the species as a random factor and the wood density class as a fixed factor. The random species effect accounts for the fact that the species were selected randomly and that several measurements were made on each species (pseudo replicates). We also tested if the average growth rate of the species we measured was correlated with their average wood density using a linear mixed model with the species as a random factor on the intercept. All the analysis were made using R software (R Core Team, 2022) and we used the "nlme" library to perform the mixed model (Pinheiro & Bates, 2000; Pinheiro et al., 2021).

3 | RESULTS

3.1 | Gas exchange

Steady-state gas exchange measurements were made following a minimum acclimation time of 20 min and up to 32 min after leaf clamping (Figure 2a). Typically, A and g_{sw} decreased shortly after clamping (21 out of 28 measurements) but some measurements also showed an increase (6 out of 28 measurements) or no change (one measurement) between initial rates and those reached at steady state. On average, the parameters g_1 and c_{g1} estimated with Equations (4) and (5) for the USO and Lamour leaf conductance models decreased from initial (~90 s) measurements to steady-state values by 30% and 22%, respectively (3.5 ± 0.4 vs 2.4 ± 0.3 $kPa^{0.5}$, $p < 0.001$ for g_1 and 0.63 ± 0.09 vs 0.49 ± 0.07 µmol^{-1} m^2 s $kPa^{0.5}$, $p = 0.005$ for c_{g1}).

The steady-state gas exchange measurements presented Figure 3 were used to evaluate the effect of wood density on the two key parameters of stomatal models, that is, g_0 and m, the intercept and slope of the plots shown in Figure 4. Regardless of the leaf conductance model we used (USO or Lamour), g_0 was not impacted by the wood density (Table 3). The stomatal slope parameter g_1 of the USO model was markedly (32%) and significantly ($p = 0.02$) lower for HWD than for LWD species (HWD = 2.50 ± 0.35, LWD = 3.70 ± 0.28). When examined with the Lamour model the stomatal slope (c_{g1}) was not significantly different ($p = 0.14$) between HWD and LWD species (HWD = 0.34 ± 0.03, LWD = 0.28 ± 0.02). This model better represented the observations (lower AIC and lower σ, Table 3).

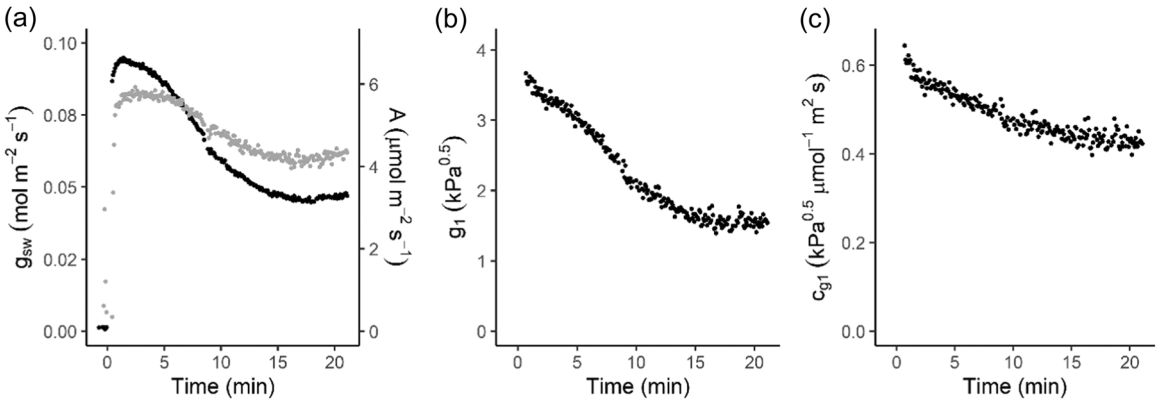

FIGURE 2 A typical plot showing the evolution of leaf gas exchange measurements following insertion of the leaf into the leaf chamber. (a) Evolution of the stomatal conductance (g_{sw}) (black dots, left y-axis) and of the photosynthesis rate (A) (grey dots, right y-axis) from insertion of the leaf to steady-state. (b) Evolution of the g_1 conductance parameter of the USO model. (c) Evolution of the c_{g1} conductance parameter of the Lamour model. USO, unified stomatal optimization.

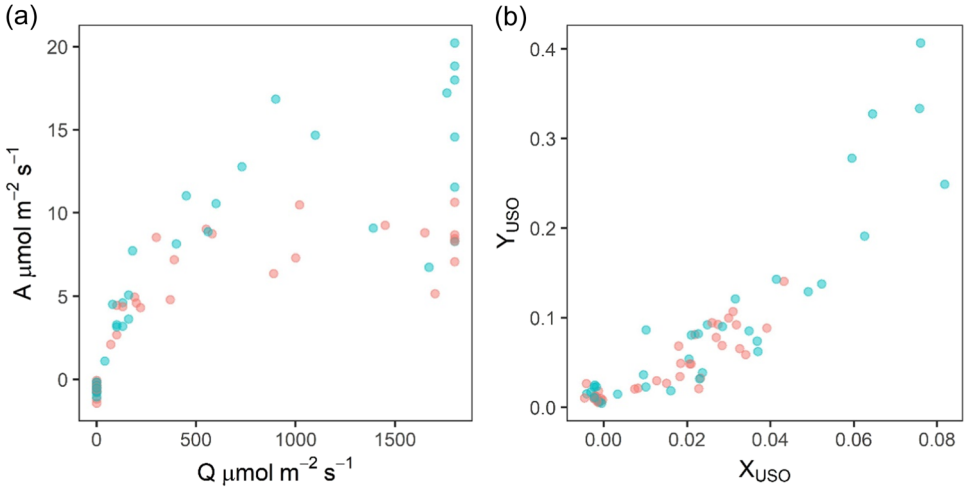

FIGURE 3 Leaf gas exchange measurements made on high wood density species (red points) and low wood density species (blue points). (a) Photosynthesis (*A*) in relation to incident irradiance at the leaf surface (*Q*). (b) Representation of the stomatal conductance response to changes in the diurnal leaf environmental conditions, where Y_{USO} represents the response variable of the USO conductance model, which is approximately equal to the stomatal conductance (Medlyn et al., 2011) and X_{USO} is determined by *A*, the CO_2 at the leaf surface, and the leaf-to-air vapour pressure deficit (Table 2, Equations 1 and 6). Each point represents a unique leaf (no repetition on the same leaf). USO, unified stomatal optimization.

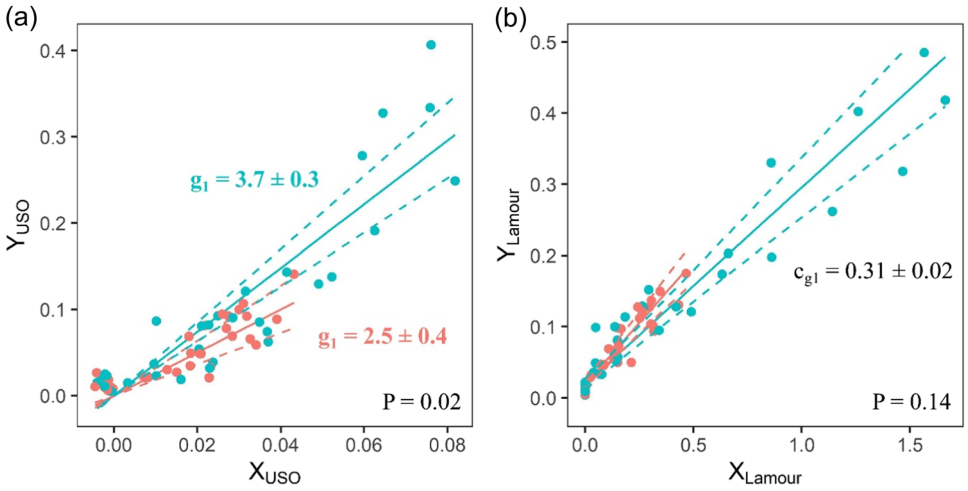

FIGURE 4 Leaf gas exchange measurements made on high wood density species (red points) and low wood density species (blue points) plotted to enable visualisation of the intercept and gradient associated with the USO (panel a) and Lamour (panels b) stomatal models. The regression lines correspond to the low wood density species (red) and high wood density species (blue) obtained using all the points. The x-axis and the y-axis correspond to the *X* and *Y* variables of the USO and Lamour models as described by Equation (6) and Table 2. The lines correspond to the mean regression and the dashed lines correspond to the confidence interval of the mean regression. The value of the slope of the regression (g_1, panel a, and c_{g1}, panel b) are added on the plots. More details on the statistics are presented in Table 3. USO, unified stomatal optimization.

We observed that the range of variation of the regressor *X* of the models differed between wood densities (x axis, Figures 3 and 4). LWD species had approximately twice the range in *X* as HWD species. Variation in *X* is dependent on VPD_{leaf}, CO_2, and *A* or $A+R_{dark}$ in the USO and Lamour models, respectively (Equations 1, 2, and 6, Table 2). The environmental conditions at the leaf surface were either held constant (CO_2 = 410 ppm) or showed little variation (VPD_{leaf} = 1.74 ± 0.14 kPa). The explanation for the higher *X* ordinate in LWD species was the observed higher photosynthetic rates at high irradiance. The A_{sat} in LWD species was almost double the rate in HWD species (15.5 ± 1.3 vs. 8.6 ± 1.5 vs. µmol m^{-2} s^{-1}, p = 0.01, Figure 3a), Similarly, $A_{sat} + R_{dark}$ in LWD species was approximately 75% greater than in HWD species (16.2 ± 1.3 vs. 9.3 ± 1.6 µmol m^{-2} s^{-1}, p = 0.01). The A_{sat} is determined by V_{cmax} and not surprisingly V_{cmax25}, as estimated by the one-point method (De Kauwe et al., 2016), was found to be markedly higher in LWD than in HWD species (LWD = 94 ± 5,

TABLE 3 Effect of the wood density on the parameters g_0 and m of the USO and Lamour conductance models (Equations 1 and 2, respectively).

Model	Obs	Wood density effect on m	g_0	σ_α	m	m HWD	m LWD	p	σ_β	σ	AIC	n
USO	All	No	0 ^{ns}	0.005	3.21*** ± 0.27	-	-	-	0.75	0.029	−271	70
USO	All	Yes	0 ^{ns}	0.005	-	2.50 ± 0.35	3.70 ± 0.28	0.02	0.42	0.029	−274	70
Lamour	All	No	0.020*** ± 0.004	0.008	0.31*** ± 0.02	-	-	-	0.06	0.019	−317	70
Lamour	All	Yes	0.019*** ± 0.004	0.008	-	0.34 ± 0.03	0.28 ± 0.02	0.14	0.04	0.020	−317	70
USO	<500	No	0.016*** ± 0.003	0.006	1.94*** ± 0.23	-	-	-	0.51	0.011	−236	43
USO	<500	Yes	0.016*** ± 0.003	0.007	-	2.02 ± 0.32	1.86 ± 0.34	0.75	0.51	0.011	−234	43
Lamour	<500	No	0.016*** ± 0.003	0.007	0.34*** ± 0.03	-	-	-	0.06	0.013	−226	43
Lamour2	<500	Yes	0.017*** ± 0.004	0.009	-	0.38 ± 0.04	0.29 ± 0.03	0.07	0.04	0.012	−227	43

Note: The results are shown when considering all the data (Obs = All) or when restricting the regression to the data measured at an irradiance below 500 µmol m^{-2} s^{-1} (Obs = <500). σ_α and σ_β represent the standard deviation of the species random effect on g_0 and on the slope parameter m which corresponds to g_1 for the unified stomatal optimization (USO) model and to c_{g1} for the Lamour model. σ is the standard deviation of the residuals. AIC is the Akaike information criterion of the model and n is the total number of leaves measured on the five low wood density species (LWD) and five high wood density species (HWD). g_0 did not vary between LWD and HWD, therefore, the mean value for both LWD and HWD species is presented (g_0). We tested if m differed between LWD and HWD species (Wood density effect on m = Yes) and gave the mean values for these two types of species in the columns "m HWD" and "m LWD". The p column gives the p-value for the difference in m between LWD and HWD species. the value of m without a wood density effect is also given in the column m (Wood density effect on m = No).

$^{*}p < 0.05$; $^{**}p < 0.01$; $^{***}p < 0.001$; ns, not significantly different from zero. For g_0 and m data are mean ± SE.

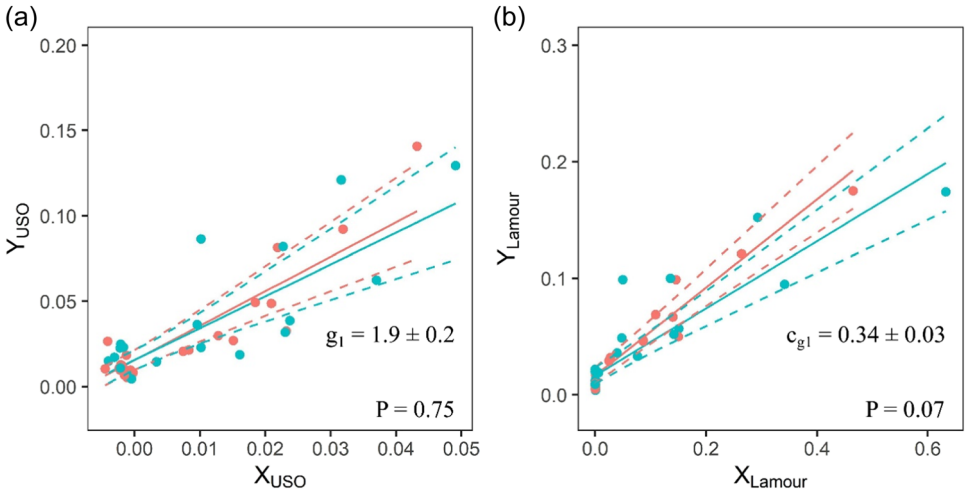

FIGURE 5 Leaf gas exchange measurements made at an irradiance below 500 µmol m^{-2} s^{-1} on high wood density species (red points) and low wood density species (blue points) plotted to enable visualisation of the intercept and gradient associated with the USO (panel a) and Lamour (panels b) stomatal models. The regression lines correspond to the low wood density species (red) and high wood density species (blue). The x-axis and the y-axis correspond to the X and Y variables, of the USO and Lamour models as described by Equation (6) and Table 2. The lines correspond to the mean regression and the dashed lines correspond to the confidence interval of the mean regression. The value of the slope of the regression (g_1, panel a, and c_{g1}, panel b) are added on the plots. More details on the statistics are presented in Table 3.

HWD = 54 ± 6 vs. µmol m^{-2} s^{-1}, $p = 0.001$, Figure 6b). R_{dark25} measured on dark-adapted leaves was 0.6 ± 0.1 µmol m^{-2} s^{-1} and did not depend on wood density ($p = 0.95$, Figure 6a).

To account for a potential bias in the estimation of the parameters g_0, g_1, and c_{g1} caused by the higher photosynthetic capacities in LWD species, and associated higher range of X values, we reanalysed the data presented in Figure 4 but restricted the sample size to a smaller data set that only included data collected under light limiting conditions. This filter ensured that the data set would be consistent with the theoretical underpinning of the USO model i.e. that the stomata optimise the electron-transport limited photosynthesis rate (Medlyn et al., 2011). Restricting the data to this subset reduced the difference

in the variation of the regressor X between wood densities (x axis, Figure 5). The estimation of g_0 and c_{g1} with the Lamour model (Table 3) stayed similar. However, with the USO model, limiting data to those collected under light limiting conditions reduced g_1 by approximately 60% ($p = 0.001$) and changed the result for the wood density effect on g_1 which was now not significant (HWD: $g_1 = 2.02 \pm 0.32$, LWD: $g_1 = 1.86 \pm 0.34$ kPa$^{0.5}$, $p = 0.75$). We note that g_0 which was not significantly different from zero when estimated with all the data, became significantly positive when we used the light limited data ($g_0 = 0.016 \pm 0.003$, $p < 0.001$) but that a higher value for g_0 did not explain the lower g_1. Indeed, fixing g_0 at zero in the mixed model (Equation 7) decreased g_1 further ($g_1 = 1.65 \pm 0.21$ [g_0 fixed to zero] vs. $g_1 = 1.95 \pm 0.23$ [free g_0]) and did not change the result of the g_1 comparison between HWD and LWD species (HWD = 1.69 ± 0.26, LWD = 1.59 ± 0.31 kPa$^{0.5}$, $p = 0.85$).

The dark-adapted $g_{sw,dark}$ was constant at 0.011 ± 0.002 mol m^{-2} s^{-1} and was not affected by WD (Figure 6c, $p = 0.25$). $g_{sw,sat}$ depended on WD and was higher in LWD than in HWD (0.29 ± 0.07 vs. 0.12 ± 0.05 mol m^{-2} s^{-1}, $p = 0.04$, Figure 6d).

3.2 | LMA, leaf N content and investment in rubisco

The mixed model using wood density as a fixed factor and species as a random effect showed no difference in LMA between the HWD and LWD species (HWD = 110.9 ± 8.1, LWD = 121.5 ± 11.4 g m^{-2}, $p = 0.38$, Figure 7a). N_{area} was not significantly different either (HWD = 2.81 ± 0.19, LWD = 2.24 ± 0.27 g m^{-2}, $p = 0.07$, Figure 7c). Estimation of the fraction of nitrogen invested in Rubisco (F_{LNR}) was approximately two times lower in HWD than in LWD (HWD = 6.4 ± 1.1%, LWD = 13.8 ± 0.9%, $p < 0.001$, Figure 6e) as a result of the lower V_{cmax25} (Figure 6b)

3.3 | Effect of the wood density on the growth rate

The growth rate of the species we studied was negatively correlated with their WD ($p = 0.02$, Figure 8). The growth rate was 0.51 ± 0.07 cm y^{-1} for a WD of 0.30 g cm^{-3} and decreased with a slope of −0.65 ± 0.20 cm y^{-1} per unit of WD for higher WD. We note that *Inga paraensis*, which is a nitrogen-fixing species, had a high growth rate despite having a HWD. Its leaf traits (LMA, N_{area}, V_{cmax25} and g_1) were however similar to the other HWD species.

4 | DISCUSSION

Accurate model representation of stomatal control is central to improved prediction of CO_2 and water fluxes, particularly in tropical forests which cycle more CO_2 and water than any other biome. Understanding how tropical forests will be affected by climate change requires representation of different PFTs in ESMs, including their different strategies associated with WUE that also impacts their vulnerability to drought. A global synthesis by Lin et al. (2015) identified a negative relationship between wood density and the g_1 parameter in the USO model. Species with a HWD had a lower g_1 and a higher WUE than species with a LWD. This finding identified an important trait-trait correlation that could advance model representation of early and late successional species which differ markedly in their wood density. When data was analysed using the USO model (Equation 1, Medlyn et al., 2011), species with a HWD had a lower g_1 (Figure 4)—consistent with the findings of Lin et al. (2015). We observed that the LWD species had a higher photosynthetic capacity than the HWD species (Figure 6b) which under high light conditions resulted in a greater range in observed A (Figure 3a). The USO model was developed with the assumption that g_{sw} is optimised to light-limited A. To evaluate if this assumption was leading to the observed difference in g_1 between LWD and HWD species we reanalysed the data using only those measurements that were collected under light limited conditions. With this limited data set the observed effect of wood density on g_1 disappeared (Figure 5), and the value of g_1 was markedly reduced. The Lamour model (Equation 2, Lamour et al., 2022a) represents a decreasing leaf-level WUE with increasing A, that is, it accounts for the curvilinear response of the USO model that can be seen in Figure 3b. When we analysed the full data set using the Lamour model, the stomatal slope parameter (c_{g1} in the Lamour model) was not significantly different between LWD and HWD species (Figure 4) and this finding was not affected when we analysed the smaller, light-limited data set (Figure 5). This work demonstrates that if ESMs implement the Lamour model, stomatal physiology could be represented with a common parameterisation for the stomatal slope parameter but that use of the USO model would require PFT specific parameterisation. Both models would require PFT specific parameterisation of V_{cmax25}.

4.1 | Similar leaf water use efficiency across species successional status

The USO model represents an optimal behaviour where stomata respond to environmental changes so they optimise the plant "economy" of resources, namely the carbon gain (A) for a given expenditure of transpired water (E) (Cowan & Farquhar, 1977). In this framework, the response of A and E is balanced such that the small change in A caused by a small change in g_{sw} is commensurate to the small change in water loss by transpiration multiplied by the carbon cost of water (λ, $\lambda = 1/WUE$, Bonan et al., 2014). A mathematical solution for g_{sw} that satisfies this balance can be investigated based on models of A (Farquhar et al., 1980) and E. Several mathematical simplifications are however necessarily made to derive a simple analytical equation (Buckley et al., 2017). The breakthrough by Medlyn et al. (2011) was to propose an analytical solution (Equation 1) to the Cowan & Farquhar (1977) theoretical framework, with stated simplifications and assumptions, that had a similar structure to previously published empirical g_{sw} models. The USO

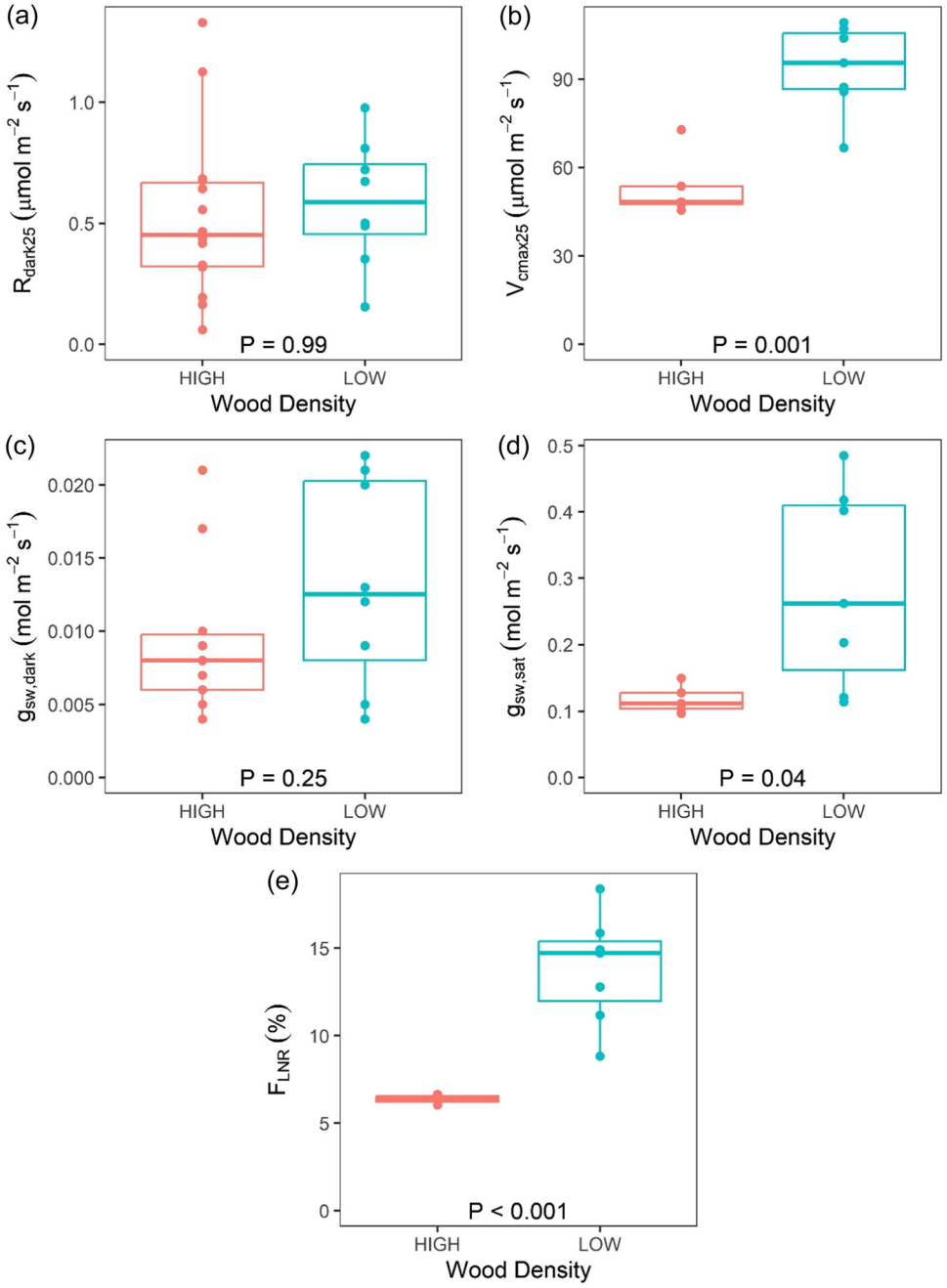

FIGURE 6 Effect of the wood density on the leaf gas exchange properties. (a) Dark-adapted respiration (R_{dark25}) measured at ambient temperature and scaled at 25°C. (b) Maximum carboxylation capacity at 25°C (V_{cmax25}) estimated from the one-point method (De Kauwe et al., 2016) using gas exchange measurements made at saturating irradiance (1800 µmol m^{-2} s^{-1}) and scaled to 25°C using a modified Arrhenius function (Leuning, 2002). (c) Steady-state leaf conductance in the dark ($g_{sw,dark}$). (d) Steady-state leaf conductance ($g_{sw,sat}$) measured at saturating irradiance. (e) Fraction of the leaf nitrogen invested in Rubisco (F_{LNR}), estimated using Equation (3). Each point represents one measurement on one leaf. The top and bottom of the boxes represent the first and third quartiles and the line is the median. The whiskers show the lowest and highest point still within 1.5x the range of the first and third quartiles.

simplifications include that the dark-respiration is zero, that photosynthesis is light-limited, and that the leaf is perfectly coupled to its environment (negligible boundary layer). In this framework and using these simplifications, the term g_1 is proportional to λ which enabled Lin et al. (2015) to make predictions of g_1 variation in different environments and different species. They predicted that dry environments should be associated with a higher carbon cost of water (higher λ, lower g_1) because water is more costly to acquire due to its scarcity. They also proposed that the water cost associated with plant's carbon requirements could be used to predict g_1. Plants with low carbon requirements for their growth should have a relatively low carbon price for water, and plants with high carbon requirement

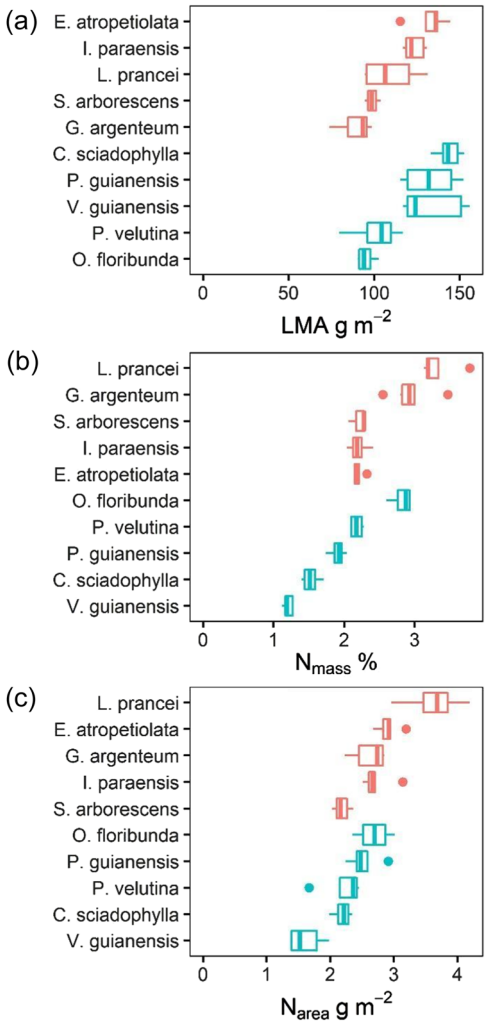

FIGURE 7 Effect of the wood density on the leaf composition of different species where the high wood density species (HWD) are in red and the low wood density species (LWD) in blue. (a) Leaf Mass per surface Area (LMA). (b) Nitrogen content expressed on a mass basis (N_{mass}). (c) Nitrogen content expressed on a surface per area basis (N_{area}). The analysis of the fixed effect of the wood density on LMA, N_{mass}, and N_{area} showed no differences between LWD and HWD species ($p > 0.05$) when accounting for the random effect of the species to consider the multiple measurements made on the same species (pseudo replicates).

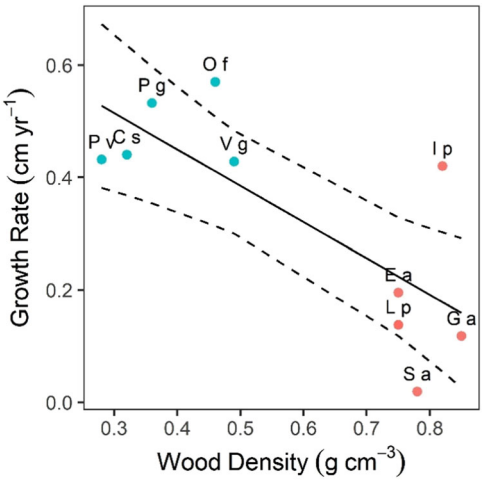

FIGURE 8 Correlation between the wood density and the growth rate of the high wood density species (in red) and the low wood density species (in blue). The wood densities were obtained from Zanne et al. (2009) and the growth rate of the trunk diameter at breast height correspond to the average value for each species calculated using the historical census data from the site. The labels correspond to the first letter of the Genus and the first letter of the species (Table 1) The line corresponds to the regression line, whereas the dotted lines represent the confidence interval of the mean when using a mixed linear model with the species as a random factor on the intercept.

should have a high carbon price for water (low g_1). Therefore g_1 should decrease with wood density, due to the higher cost of wood construction per unit water transported (Héroult et al., 2013; Lin et al., 2015). Here, we tried to evaluate this hypothesis while avoiding possible confounding effect associated with different environmental conditions by choosing co-occurring species in the same forest. We did not observe the expected negative correlation between wood density and g_1 when limiting the data set to observations collected when A was light limited (Figure 5). This could potentially be attributed to a lack of correlation between wood density and the efficiency of water transport in the studied species (Chave et al., 2009; Mujawamariya et al., 2023; Poorter et al., 2010; Zanne et al., 2010) as well as variation in the allocation of carbon for acquiring and transporting water in the roots and stem.

The Lamour et al. (2022a) conductance model is empirical. In contrast to the USO model it is not built based on an optimality framework but was proposed to consider the empirical observation that g_{sw} responds nonlinearly to changes in A when VPD_{leaf} and CO_2 are constant. This nonlinear relationship biased the estimation of g_1 in the USO model which depended on the irradiance and A in tropical species (Lamour et al., 2022a). Here, we observed the same phenomena where g_1 in the USO model was markedly lower when we considered only the gas exchange measurements made below an irradiance of 500 µmol m^{-2} s^{-1} (Table 3). The difference between observations and the USO model could be due to several factor, including an incorrect optimality premise (Anderegg et al., 2018; Buckley, 2021; Prentice et al., 2014; Resco de Dios et al., 2020; Wolf et al., 2016); or unrealistic mathematical simplifications (Buckley et al., 2017; Huang et al., 2021). Lamour et al. (2022a) proposed that the nonlinearity at low light levels could be due to a nonoptimal behaviour and that the nonlinearity at high light level could be due to the transition between light-limited and light-saturated photosynthesis. Indeed, previous work that represented these limitations accounted for some of the nonlinearity (Buckley et al., 2017). The negligible boundary layer assumption could also bias predictions by the USO model. It is unlikely that the boundary layer is negligible in most ecosystems and T_{leaf} is often different from T_{air} (Still et al., 2022), including at this site (Gimenez et al., 2019). To our knowledge, the

effect this could possibly have on the USO model predictions has not been investigated. Despite its empirical nature, the Lamour et al. (2022a) model has value due to its ability to closely match field-based observations across a wide range of environmental conditions (Table 3, lower AIC, lower σ).

The minimum conductance in leaves ($g_{sw,dark}$) is assumed to be caused by imperfectly closed stomata as well as non-negligible cuticular conductance (Duursma et al., 2019; Lamour et al., 2022b; Márquez et al., 2021; Slot et al., 2021) and may be a key trait for explaining plant vulnerability to drought in addition to other traits such as the xylem vulnerability to cavitation, leaf deciduousness, or nonstructural carbohydrate storage (Choat et al., 2018; Cochard, 2021; Maréchaux et al., 2015; Martin-StPaul et al., 2017; McDowell et al., 2018; O'Brien et al., 2014). LWD and HWD species had similar $g_{sw,dark}$ in this forest. This suggests that the increased mortality of LWD trees in the BIONTE experiment in drought years (Chambers et al. in prep) was not attributable to a higher water loss in leaves with closed stomata, a trait represented in ESMs by the g_0 parameter (Lombardozzi et al., 2017). Note that a recent study in a tropical forest showed that the cuticular conductance, a component of $g_{sw,dark}$ and g_0, was generally higher in deciduous than in evergreen species, and in species with leaf trichomes, but that the cuticular conductance was highly variable among species (Slot et al., 2021).

4.2 | Higher investments in rubisco capacity in early successional species

We showed that V_{cmax25} is markedly lower in HWD than in LWD species, consistent with other experimental studies in tropical forests (Bonal et al., 2007; Dusenge et al., 2015; Mujawamariya et al., 2023; Nogueira et al., 2004; Raaimakers et al., 1995; Reich et al., 1995; Ziegler et al., 2020). Despite the differences in V_{cmax25}, we showed no difference in N_{area} and therefore, following the trend in V_{cmax25}, the F_{LNR} was approximately double in LWD species. Rubisco is the most abundant protein in leaves and represents a significant allocation of leaf nitrogen (Evans & Clarke, 2019). Here we see that the fraction of leaf N invested in Rubisco is lower in HWD species, a similar result as in African montane tropical species (Dusenge et al., 2015; Ziegler et al., 2020). This implies that the proportion of the nitrogen invested in other proteins and leaf constituents that could be used for defense, is greater in HWD species than LWD species. This is consistent with higher leaf longevity and a greater resistance to biotic and abiotic stress that has been previously observed in the leaves of HWD species (Coley & Barone, 1996; Onoda et al., 2017). The higher photosynthetic capacity of the LWD species is a key attribute of the succession theory and is thought to explain their fast growth rates that we also observed at this field site (Kunstler et al., 2015).

We showed that R_{dark25} was not different for LWD and HWD species. This is consistent with the absence of difference in N_{area} between LWD and HWD species. Indeed; R_{dark25} is thought to scale with N_{area} since N_{area} is a good proxy for the amount of total protein in the leaf that needs to be repaired and replaced by processes fuelled by respiratory metabolism (Reich et al., 2008). In ESMs, R_{dark25} is generally assumed to be 1.5% of V_{cmax25} (Clark et al., 2011; Oleson et al., 2013). Here, we see that this assumption would markedly overestimate R_{dark25} in LWD species (1.4 ± 0.1 µmol m^{-2} s^{-1} estimated R_{dark25}, vs. 0.6 ± 0.1 µmol m^{-2} s^{-1} observed R_{dark25}) but be quite reasonable for the HWD species (0.8 ± 0.1 µmol m^{-2} s^{-1} estimated vs. 0.6 ± 0.1 µmol m^{-2} s^{-1} observed). Recent work showed that better representation of R_{dark25} is needed in ESMs (Bruhn et al., 2022; Lamour et al., 2023a; Souza et al., 2021; Weerasinghe et al., 2014; Ziegler et al., 2020), and our results support this.

4.3 | Effect of the waiting time since clamping on the estimation of leaf water use efficiency

Measurement of the stomatal slope parameter is fraught with trade-offs and compromises and a number of approaches have been used to estimate this important physiological parameter (Ball et al., 1987; Bernacchi et al., 2006; Davidson et al., 2023; Medlyn et al., 2011; Miner et al., 2017; Wu et al., 2020). Here, using an in situ steady-state-survey approach—enabled by canopy access and typically low wind speeds at the field site—we showed that the time since inserting a leaf into the leaf chamber impacted A and g_{sw} and that the leaf-WUE was higher (lower m) when measured at steady-state compared with measurements made within 90 s of inserting the leaf (Figure 2). Most of the survey-type gas exchange measurements are made after a short acclimation time, typically less than 90 s (Bernacchi et al., 2006; Davidson et al., 2023; Leakey et al., 2006; Lin et al., 2015; Wu et al., 2020). However, it is known that stomata react more slowly to changes at the leaf surface than photosynthesis (Lawson & Vialet-Chabrand, 2018). This temporal-decoupling of measured A and g_{sw}—and the unavoidable mismatch between environmental conditions in the leaf chamber and in the open canopy—led us to hypothesise that a calculation of the stomatal slope parameter from data collected using typical survey style measurements that are completed within 90 s would differ from estimations of the stomatal slope parameter made under steady-state gas exchange conditions.

The assumption made in rapid survey measurements is that the conditions at the leaf surface in the gas exchange instrument match those in the natural environment immediately before clamping and that, even if there is some error associated with matching ambient conditions that should not lead to a systematic bias on the derived parameters (Davidson et al., 2023; Miner et al., 2017). However, some of the changes imposed by leaf gas exchange instruments are systematic and usually have nonlinear and interactive effects on the variables used to estimate m (Equations 1 and 2), which challenge this assumption. Let's consider some key environmental variables. The boundary layer is destroyed by the mixing fan which creates strong air turbulence at the leaf surface (von Caemmerer & Farquhar, 1981; Long et al., 1996), in sharp contrast to ambient conditions (the wind speeds observed during our measurements were low, generally 0 and

up to 2 m s^{-1}, data not shown). Even if we assume that the incident irradiance is accurately matched to prevailing environmental conditions, clamping a leaf in the instrument alters the light quality compared to natural light. Both the spectral distribution of the light (e.g., 90% red and 10% blue in our study) and the fraction of direct and diffuse light are modified by the artificial source (Berry et al., 2022; Zhen et al., 2022). The leaf energy budget is modified as a result of using an artificial "cold" light source and the mixing fan. It is not possible to simultaneously control T_{leaf}, T_{air}, and the relative humidity in the instrument so that they all match the natural environment. Here, we chose to control the air temperature inside the instrument, so it was the same as ambient and limited modification of the relative humidity of the air that entered the leaf chamber. These choices are common in leaf gas exchange studies (Bernacchi et al., 2006; Leakey et al., 2006; Wu et al., 2020), but it is likely that T_{leaf} and VPD_{leaf} differed between the leaf chamber and the natural environment. Both variables affect the stomatal response, and the calculation of m. Changes in VPD_{leaf} are known to rapidly change stomatal conductance in the "wrong" way, meaning that conductance transiently and rapidly increases when the VPD_{leaf} increases, before finally decreasing (and vice versa when the VPD_{leaf} decreases, Buckley, 2019; McAdam & Brodribb, 2015, 2016). We believe that estimating the stomatal slope parameter from steady-state gas exchange data collected as either independent survey style measurements or as part of a response curve is the most appropriate approach (Davidson et al., 2023; Lamour et al., 2022a; Leakey et al., 2006; McAdam & Brodribb, 2015).

ACKNOWLEDGMENTS

This work was supported by the Next-Generation Ecosystem Experiments—Tropics Project that is supported by the Office of Biological and Environmental Research in the Department of Energy, Office of Science, and through the United States Department of Energy contract No. DE-SC0012704 to Brookhaven National Laboratory.

DATA AVAILABILITY STATEMENT

The data that support the findings of this study are openly available in the NGEE Tropics Data Collection at https://doi.org/10.15486/ngt/1923654, reference number NGT0197 (Lamour et al., 2023b).

ORCID

Julien Lamour http://orcid.org/0000-0002-4410-507X
Daisy C. Souza http://orcid.org/0000-0001-5522-6494
Bruno O. Gimenez http://orcid.org/0000-0001-7336-9448
Niro Higuchi http://orcid.org/0000-0002-1203-4502
Jérôme Chave http://orcid.org/0000-0002-7766-1347
Jeffrey Chambers http://orcid.org/0000-0003-3983-7847
Alistair Rogers http://orcid.org/0000-0001-9262-7430

REFERENCES

Akaike, H. (1974) A new look at the statistical model identification. *IEEE Transactions on Automatic Control*, 19, 716–723.
Amaral, M., Lima, A., Higuchi, F., dos Santos, J. & Higuchi, N. (2019) Dynamics of tropical forest twenty-five years after experimental logging in central Amazon mature forest. *Forests*, 10, 89.
Anderegg, W.R.L., Wolf, A., Arango-Velez, A., Choat, B., Chmura, D.J., Jansen, S. et al. (2018) Woody plants optimise stomatal behaviour relative to hydraulic risk. *Ecology Letters*, 21, 968–977.
Apgaua, D.M.G., Tng, D.Y.P., Cernusak, L.A., Cheesman, A.W., Santos, R.M., Edwards, W.J. et al. (2017) Plant functional groups within a tropical forest exhibit different wood functional anatomy. *Functional Ecology*, 31, 582–591.
Asner, G.P., Knapp, D.E., Broadbent, E.N., Oliveira, P.J.C., Keller, M. & Silva, J.N. (2005) Selective logging in the Brazilian Amazon. *Science*, 310, 480–482.
Ball, J.T., Woodrow, I.E. & Berry, J.A. (1987). A model predicting stomatal conductance and its contribution to the control of photosynthesis under different environmental conditions. In: Biggins, J. ed. Progress in photosynthesis research: Volume 4 Proceedings of the VIIth International Congress on Photosynthesis Providence, Rhode Island, USA, August 10–15, 1986. Dordrecht: Springer Netherlands, p. 221–224.
Bazzaz, F.A. & Pickett, S.T.A. (1980) Physiological ecology of tropical succession: a comparative review. *Annual Review of Ecology and Systematics*, 11, 287–310.
Beer, C., Reichstein, M., Tomelleri, E., Ciais, P., Jung, M., Carvalhais, N. et al. (2010) Terrestrial gross carbon dioxide uptake: global distribution and covariation with climate. *Science*, 329, 834–838.
Bernacchi, C.J., Leakey, A.D., Heady, L.E., Morgan, P.B., Dohleman, F.G., McGrath, J.M. et al. (2006) Hourly and seasonal variation in photosynthesis and stomatal conductance of soybean grown at future CO2 and ozone concentrations for 3 years under fully open-air field conditions. *Plant, Cell & Environment*, 29, 2077–2090.
Bernacchi, C.J., Singsaas, E.L., Pimentel, C., Portis Jr., A.R. & Long, S.P. (2001) Improved temperature response functions for models of rubisco-limited photosynthesis. *Plant, Cell & Environment*, 24, 253–259.
Berry, Z.C., Larue, J. & Goldsmith, G.R. (2022) Quantifying and manipulating the angles of light in experimental measurements of plant gas exchange. *Plant, Cell & Environment*, 45, 1954–1961.
Bonal, D., Born, C., Brechet, C., Coste, S., Marcon, E., Roggy, J.-C. et al. (2007) The successional status of tropical rainforest tree species is associated with differences in leaf carbon isotope discrimination and functional traits. *Annals of Forest Science*, 64, 169–176.
Bonan, G.B., Lawrence, P.J., Oleson, K.W., Levis, S., Jung, M., Reichstein, M. et al. (2011) Improving canopy processes in the community land model version 4 (CLM4) using global flux fields empirically inferred from FLUXNET data. *Journal of Geophysical Research*, 116, G02014.
Bonan, G.B., Williams, M., Fisher, R.A. & Oleson, K.W. (2014) Modeling stomatal conductance in the earth system: linking leaf water-use efficiency and water transport along the soil–plant–atmosphere continuum. *Geoscientific Model Development*, 7, 2193–2222.
Bruhn, D., Newman, F., Hancock, M., Povlsen, P., Slot, M., Sitch, S. et al. (2022) Nocturnal plant respiration is under strong non-temperature control. *Nature Communications*, 13, 5650.
Buckley, T.N. (2019) How do stomata respond to water status? *New Phytologist*, 224, 21–36.
Buckley, T.N. (2021) Optimal carbon partitioning helps reconcile the apparent divergence between optimal and observed canopy profiles of photosynthetic capacity. *New Phytologist*, 230, 2246–2260.
Buckley, T.N., Sack, L. & Farquhar, G.D. (2017) Optimal plant water economy. *Plant, Cell & Environment*, 40, 881–896.
Burnett, A.C., Davidson, K.J., Serbin, S.P. & Rogers, A. (2019) The "one-point method" for estimating maximum carboxylation capacity of photosynthesis: a cautionary tale. *Plant, Cell & Environment*, 42, 2472–2481.

von Caemmerer, S., & Farquhar, G. D. (1981) Some relationships between the biochemistry of photosynthesis and the gas exchange of leaves. *Planta*, 153(4), 376–386. https://doi.org/10.1007/bf00384257

Chave, J., Coomes, D., Jansen, S., Lewis, S.L., Swenson, N.G. & Zanne, A.E. (2009) Towards a worldwide wood economics spectrum. *Ecology Letters*, 12, 351–366.

Chazdon, R.L., Broadbent, E.N., Rozendaal, D.M.A., Bongers, F., Zambrano, A.M.A., Aide, T.M. et al. (2016) Carbon sequestration potential of second-growth forest regeneration in the latin American tropics. *Science Advances*, 2, e1501639.

Choat, B., Brodribb, T.J., Brodersen, C.R., Duursma, R.A., López, R. & Medlyn, B.E. (2018) Triggers of tree mortality under drought. *Nature*, 558, 531–539.

Clark, D.B., Mercado, L.M., Sitch, S., Jones, C.D., Gedney, N., Best, M.J. et al. (2011) The joint UK land environment simulator (JULES), model description – part 2: carbon fluxes and vegetation dynamics. *Geoscientific Model Development*, 4, 701–722.

Cochard, H. (2021) A new mechanism for tree mortality due to drought and heatwaves. *Peer Community Journal*, 1, e36.

Coley, P.D. & Barone, J.A. (1996) Herbivory and plant defenses in tropical forests. *Annual Review of Ecology and Systematics*, 27, 305–335.

Cowan, I.R. & Farquhar, G.D. (1977) Stomatal function in relation to leaf metabolism and environment. *Symposia of the Society for Experimental Biology*, 31, 471–505.

Davidson, K.J., Lamour, J., Rogers, A., Ely, K.S., Li, Q., McDowell, N.G. et al. (2023) Short-term variation in leaf-level water use efficiency in a tropical forest. *New Phytologist*, 237, 2069–2087.

Davidson, K.J., Lamour, J., Rogers, A. & Serbin, S.P. (2022) Late-day measurement of excised branches results in uncertainty in the estimation of two stomatal parameters derived from response curves in *Populus deltoides* bartr. × *Populus nigra* L. *Tree Physiology*, 42, 1377–1395.

DeArmond, D., Emmert, F., Lima, A.J.N. & Higuchi, N. (2019) Impacts of soil compaction persist 30 years after logging operations in the Amazon basin. *Soil and Tillage Research*, 189, 207–216.

Dewar, R., Mauranen, A., Mäkelä, A., Hölttä, T., Medlyn, B. & Vesala, T. (2018) New insights into the covariation of stomatal, mesophyll and hydraulic conductances from optimization models incorporating nonstomatal limitations to photosynthesis. *New Phytologist*, 217, 571–585.

Dietze, M.C., Serbin, S.P., Davidson, C., Desai, A.R., Feng, X., Kelly, R. et al. (2014) A quantitative assessment of a terrestrial biosphere model's data needs across north American biomes: PEcAn/ED model-data uncertainty analysis. *Journal of Geophysical Research: Biogeosciences*, 119, 286–300.

Dusenge, M.E., Wallin, G., Gårdesten, J., Niyonzima, F., Adolfsson, L., Nsabimana, D. et al. (2015) Photosynthetic capacity of tropical montane tree species in relation to leaf nutrients, successional strategy and growth temperature. *Oecologia*, 177, 1183–1194.

Duursma, R.A., Blackman, C.J., Lopéz, R., Martin-StPaul, N.K., Cochard, H. & Medlyn, B.E. (2019) On the minimum leaf conductance: its role in models of plant water use, and ecological and environmental controls. *New Phytologist*, 221, 693–705.

Evans, J.R. & Clarke, V.C. (2019) The nitrogen cost of photosynthesis. *Journal of Experimental Botany*, 70, 7–15.

Farquhar, G.D., von Caemmerer, S. & Berry, J.A. (1980) A biochemical model of photosynthetic CO_2 assimilation in leaves of C3 species. *Planta*, 149, 78–90.

Fisher, J.B., Huntzinger, D.N., Schwalm, C.R. & Sitch, S. (2014) Modeling the terrestrial biosphere. *Annual Review of Environment and Resources*, 39, 91–123.

Fisher, R.A., Koven, C.D., Anderegg, W.R.L., Christoffersen, B.O., Dietze, M.C., Farrior, C.E. et al. (2018) Vegetation demographics in earth system models: a review of progress and priorities. *Global Change Biology*, 24, 35–54.

Franklin, O., Harrison, S.P., Dewar, R., Farrior, C.E., Brännström, Å., Dieckmann, U. et al. (2020) Organizing principles for vegetation dynamics. *Nature Plants*, 6, 444–453.

Franks, P.J., Bonan, G.B., Berry, J.A., Lombardozzi, D.L., Holbrook, N.M., Herold, N. et al. (2018) Comparing optimal and empirical stomatal conductance models for application in earth system models. *Global Change Biology*, 24, 5708–5723.

Friedlingstein, P., O'Sullivan, M., Jones, M.W., Andrew, R.M., Gregor, L., Hauck, J. et al. (2022) Global carbon budget 2022. *Earth System Science Data*, 14, 4811–4900.

Gaui, T.D., Costa, F.R.C., Coelho de Souza, F., Amaral, M.R.M., de Carvalho, D.C., Reis, F.Q. et al. (2019) Long-term effect of selective logging on floristic composition: a 25 year experiment in the Brazilian Amazon. *Forest Ecology and Management*, 440, 258–266.

Gimenez, B.O., Jardine, K.J., Higuchi, N., Negrón-Juárez, R.I., Sampaio-Filho, I.J. & Cobello, L.O. et al. (2019) Species-Specific shifts in diurnal sap velocity dynamics and hysteretic behavior of ecophysiological variables during the 2015–2016 el niño event in the Amazon forest. *Frontiers in Plant Science*, 10, 830.

Hasper, T.B., Dusenge, M.E., Breuer, F., Uwizeye, F.K., Wallin, G. & Uddling, J. (2017) Stomatal CO_2 responsiveness and photosynthetic capacity of tropical woody species in relation to taxonomy and functional traits. *Oecologia*, 184, 43–57.

Héroult, A., Lin, Y.-S., Bourne, A., Medlyn, B.E. & Ellsworth, D.S. (2013) Optimal stomatal conductance in relation to photosynthesis in climatically contrasting eucalyptus species under drought. *Plant, Cell & Environment*, 36, 262–274.

Higuchi, N., dos Santos, J., Ribeiro, J., Freitas, J., Vieira, G. & Cöic, L. (1997). Biomassa e nutrientes florestais–relatório final do projeto bionte. *Final Report, Manaus*.

Huang, G., Yang, Y., Zhu, L., Peng, S. & Li, Y. (2021) Temperature responses of photosynthesis and stomatal conductance in rice and wheat plants. *Agricultural and Forest Meteorology*, 300, 108322.

Huc, R., Ferhi, A. & Guehl, J.M. (1994) Pioneer and late stage tropical rainforest tree species (French Guiana) growing under common conditions differ in leaf gas exchange regulation, carbon isotope discrimination and leaf water potential. *Oecologia*, 99, 297–305.

Jakovac, C.C., Meave, J.A., Bongers, F., Letcher, S.G., Dupuy, J.M., Piotto, D. et al. (2022) Strong floristic distinctiveness across neotropical successional forests. *Science Advances*, 8, eabn1767.

Jasechko, S., Sharp, Z.D., Gibson, J.J., Birks, S.J., Yi, Y. & Fawcett, P.J. (2013) Terrestrial water fluxes dominated by transpiration. *Nature*, 496, 347–350.

De Kauwe, M.G., Kala, J., Lin, Y.-S., Pitman, A.J., Medlyn, B.E., Duursma, R.A. et al. (2015) A test of an optimal stomatal conductance scheme within the CABLE land surface model. *Geoscientific Model Development*, 8, 431–452.

De Kauwe, M.G., Lin, Y.-S., Wright, I.J., Medlyn, B.E., Crous, K.Y., Ellsworth, D.S. et al. (2016) A test of the 'one-point method' for estimating maximum carboxylation capacity from field-measured, light-saturated photosynthesis. *New Phytologist*, 210, 1130–1144.

Knauer, J., Werner, C. & Zaehle, S. (2015) Evaluating stomatal models and their atmospheric drought response in a land surface scheme: a multibiome analysis. *Journal of Geophysical Research: Biogeosciences*, 120, 1894–1911.

Kunstler, G., Falster, D., Coomes, D. A., Hui, F., Kooyman, R. M., Laughlin, D. C. et al. (2015) Plant functional traits have globally consistent effects on competition. *Nature*, 529(7585), 204–207. https://doi.org/10.1038/nature16476

Lamour, J., Davidson, K.J., Ely, K.S., Li, Q., Serbin, S.P. & Rogers, A. (2022b) New calculations for photosynthesis measurement systems: what's the impact for physiologists and modelers? *New Phytologist*, 233, 592–598.

Lamour, J., Davidson, K.J., Ely, K.S., Le Moguédec, G., Anderson, J.A., Li, Q. et al. (2023a) The effect of the vertical gradients of photosynthetic parameters on the CO_2 assimilation and transpiration of a Panamanian tropical forest. *New Phytologist*, 238, 2345–2362.

Lamour, J., Davidson, K.J., Ely, K.S., Le Moguédec, G., Leakey, A.D.B., Li, Q. et al. (2022a) An improved representation of the relationship between photosynthesis and stomatal conductance leads to more stable estimation of conductance parameters and improves the goodness-of-fit across diverse data sets. *Global Change Biology*, 28, 3537–3556.

Lamour, J., Souza, D.C., Gimenez, B.O., Plácido, A.D.L., Rodrigues de Oliveira, L. & Rogers, A. (2023b). Leaf gas exchange, spectral reflectance and leaf composition, BIONTE, Brazil, 2022. v 1.0. https://doi.org/10.15486/ngt/1923654

Lawson, T. & Vialet-Chabrand, S. (2018) Speedy stomata, photosynthesis and plant water use efficiency. *New Phytologist*, 221(1), 93–98. https://doi.org/10.1111/nph.15330

Leakey, A.D., Bernacchi, C.J., Ort, D.R. & Long, S.P. (2006) Long-term growth of soybean at elevated [CO_2] does not cause acclimation of stomatal conductance under fully open-air conditions. *Plant, Cell & Environment*, 29, 1794–1800.

Leuning, R. (2002) Temperature dependence of two parameters in a photosynthesis model. *Plant, Cell & Environment*, 25, 1205–1210.

Li, Q., Serbin, S.P., Lamour, J., Davidson, K.J., Ely, K.S. & Rogers, A. (2022) Implementation and evaluation of the unified stomatal optimization approach in the functionally assembled terrestrial ecosystem simulator (FATES). *Geoscientific Model Development*, 15, 4313–4329.

Lin, Y.-S., Medlyn, B.E., Duursma, R.A., Prentice, I.C., Wang, H., Baig, S. et al. (2015) Optimal stomatal behaviour around the world. *Nature Climate Change*, 5, 459–464.

Lombardozzi, D.L., Zeppel, M.J.B., Fisher, R.A. & Tawfik, A. (2017) Representing nighttime and minimum conductance in CLM4.5: global hydrology and carbon sensitivity analysis using observational constraints. *Geoscientific Model Development*, 10, 321–331.

Long, S. P., Farage, P. K. & Garcia, R. L. (1996) Measurement of leaf and canopy photosynthetic CO_2 exchange in the field. *Journal of Experimental Botany*, 47(11), 1629–1642. https://doi.org/10.1093/jxb/47.11.1629

Maréchaux, I., Bartlett, M.K., Sack, L., Baraloto, C., Engel, J., Joetzjer, E. et al. (2015) Drought tolerance as predicted by leaf water potential at turgor loss point varies strongly across species within an amazonian forest. *Functional Ecology*, 29, 1268–1277.

Márquez, D.A., Stuart-Williams, H. & Farquhar, G.D. (2021) An improved theory for calculating leaf gas exchange more precisely accounting for small fluxes. *Nature Plants*, 7, 317–326.

Martin-StPaul, N., Delzon, S. & Cochard, H. (2017) Plant resistance to drought depends on timely stomatal closure. *Ecology Letters*, 20, 1437–1447.

McAdam, S.A.M. & Brodribb, T.J. (2015) The evolution of mechanisms driving the stomatal response to vapor pressure deficit. *Plant Physiology*, 167, 833–843.

McAdam, S.A.M. & Brodribb, T.J. (2016) Linking turgor with ABA biosynthesis: implications for stomatal responses to vapor pressure deficit across land plants. *Plant Physiology*, 171, 2008–2016.

McDowell, N., Allen, C.D., Anderson-Teixeira, K., Brando, P., Brienen, R., Chambers, J. et al. (2018) Drivers and mechanisms of tree mortality in moist tropical forests. *New Phytologist*, 219, 851–869.

Medlyn, B.E., Duursma, R.A., Eamus, D., Ellsworth, D.S., Prentice, I.C., Barton, C.V.M. et al. (2011) Reconciling the optimal and empirical approaches to modelling stomatal conductance. *Global Change Biology*, 17, 2134–2144.

Medlyn, B.E., De Kauwe, M.G., Lin, Y.-S., Knauer, J., Duursma, R.A., Williams, C.A. et al. (2017) How do leaf and ecosystem measures of water-use efficiency compare? *New Phytologist*, 216, 758–770.

Meng, L., Chambers, J., Koven, C., Pastorello, G., Gimenez, B., Jardine, K. et al. (2022) Soil moisture thresholds explain a shift from light-limited to water-limited sap velocity in the central Amazon during the 2015–16 el niño drought. *Environmental Research Letters*, 17, 064023.

Migliavacca, M., Musavi, T., Mahecha, M.D., Nelson, J.A., Knauer, J., Baldocchi, D.D. et al. (2021) The three major axes of terrestrial ecosystem function. *Nature*, 598, 468–472.

Mills, M.B., Malhi, Y., Ewers, R.M., Kho, L.K., Teh, Y.A., Both, S. et al. (2023) Tropical forests post-logging are a persistent net carbon source to the atmosphere. *Proceedings of the National Academy of Sciences*, 120, e2214462120.

Miner, G.L., Bauerle, W.L. & Baldocchi, D.D. (2017) Estimating the sensitivity of stomatal conductance to photosynthesis: a review. *Plant, Cell & Environment*, 40, 1214–1238.

Mujawamariya, M., Wittemann, M., Dusenge, M.E., Manishimwe, A., Ntirugulirwa, B., Zibera, E. et al. (2023) Contrasting warming responses of photosynthesis in early- and late-successional tropical trees. *Tree Physiology*, 43, 1104–1117.

Nogueira, A., Martinez, C.A., Ferreira, L.L. & Prado, C.H.B.A. (2004) Photosynthesis and water use efficiency in twenty tropical tree species of differing succession status in a Brazilian reforestation. *Photosynthetica*, 42, 351–356.

Nyirambangutse, B., Zibera, E., Uwizeye, F.K., Nsabimana, D., Bizuru, E., Pleijel, H. et al. (2017) Carbon stocks and dynamics at different successional stages in an afromontane tropical forest. *Biogeosciences*, 14, 1285–1303.

O'Brien, M.J., Leuzinger, S., Philipson, C.D., Tay, J. & Hector, A. (2014) Drought survival of tropical tree seedlings enhanced by non-structural carbohydrate levels. *Nature Climate Change*, 4, 710–714.

Oleson, K., Lawrence, D., Bonan, G., Drewniak, B., Huang, M., Koven, C. et al. (2013) *Technical description of version 4.5 of the Community Land Model (CLM)*. Boulder, Colorado, US: NCAR Technical Notes.

Oliveira, R.S., Eller, C.B., Barros, F.V., Hirota, M., Brum, M. & Bittencourt, P. (2021) Linking plant hydraulics and the fast–slow continuum to understand resilience to drought in tropical ecosystems. *New Phytologist*, 230, 904–923.

Oliver, R.J., Mercado, L.M., Sitch, S., Simpson, D., Medlyn, B.E., Lin, Y.-S. et al. (2018) Large but decreasing effect of ozone on the european carbon sink. *Biogeosciences*, 15, 4245–4269.

Onoda, Y., Wright, I.J., Evans, J.R., Hikosaka, K., Kitajima, K., Niinemets, Ü. et al. (2017) Physiological and structural tradeoffs underlying the leaf economics spectrum. *New Phytologist*, 214, 1447–1463.

Ordway, E.M. & Asner, G.P. (2020) Carbon declines along tropical forest edges correspond to heterogeneous effects on canopy structure and function. *Proceedings of the National Academy of Sciences*, 117, 7863–7870.

Pinheiro, J. & Bates, D. (2000) *Mixed-effects models in S and S-PLUS*. New-York: Springer Science & Business Media.

Pinheiro, J., Bates, D., DebRoy, S. & Sarkar, D., R Core Team. (2021) nlme: linear and nonlinear mixed effects models.

Poorter, L., Bongers, F., Aide, T.M., Almeyda Zambrano, A.M., Balvanera, P., Becknell, J.M. et al. (2016) Biomass resilience of neotropical secondary forests. *Nature*, 530, 211–214.

Poorter, L., McDonald, I., Alarcón, A., Fichtler, E., Licona, J.-C., Peña-Claros, M. et al. (2010) The importance of wood traits and hydraulic conductance for the performance and life history strategies of 42 rainforest tree species. *New Phytologist*, 185, 481–492.

Poorter, L., Rozendaal, D.M.A., Bongers, F., de Almeida-Cortez, J.S., Almeyda Zambrano, A.M., Álvarez, F.S. et al. (2019) Wet and dry tropical forests show opposite successional pathways in wood density but converge over time. *Nature Ecology & Evolution*, 3, 928–934.

Poulter, B., Ciais, P., Hodson, E., Lischke, H., Maignan, F., Plummer, S. et al. (2011) Plant functional type mapping for earth system models. *Geoscientific Model Development*, 4, 993–1010.

Prentice, I.C., Dong, N., Gleason, S.M., Maire, V. & Wright, I.J. (2014) Balancing the costs of carbon gain and water transport: testing a new theoretical framework for plant functional ecology. *Ecology Letters*, 17, 82–91.

R Core Team. (2022) *R: A language and environment for statistical computing*. Vienna, Austria: R Foundation for Statistical Computing.

Raaimakers, D., Boot, R.G.A., Dijkstra, P. & Pot, S. (1995) Photosynthetic rates in relation to leaf phosphorus content in pioneer versus climax tropical rainforest trees. *Oecologia*, 102, 120–125.

Rangel Pinagé, E., Keller, M., Duffy, P., Longo, M., Dos-Santos, M. & Morton, D. (2019) Long-term impacts of selective logging on Amazon forest dynamics from multi-temporal airborne LiDAR. *Remote Sensing*, 11, 709.

Rangel Pinagé, E., M. Bell, D., Longo, M., Gao, S., Keller, M., Silva, C.A. et al. (2022) Forest structure and solar-induced fluorescence across intact and degraded forests in the Amazon. *Remote Sensing of Environment*, 274, 112998.

Reich, P.B. (2014) The world-wide 'fast–slow' plant economics spectrum: a traits manifesto. *Journal of Ecology*, 102, 275–301.

Reich, P.B., Ellsworth, D.S. & Uhl, C. (1995) Leaf carbon and nutrient assimilation and conservation in species of differing successional status in an oligotrophic amazonian forest. *Functional Ecology*, 9, 65–76.

Reich, P.B., Tjoelker, M.G., Pregitzer, K.S., Wright, I.J., Oleksyn, J. & Machado, J.-L. (2008) Scaling of respiration to nitrogen in leaves, stems and roots of higher land plants. *Ecology Letters*, 11, 793–801.

Reich, P.B., Uhl, C., Walters, M.B. & Ellsworth, D.S. (1991) Leaf lifespan as a determinant of leaf structure and function among 23 amazonian tree species. *Oecologia*, 86, 16–24.

Resco de Dios, V., Anderegg, W.R.L., Li, X., Tissue, D.T., Bahn, M., Landais, D. et al. (2020) Circadian regulation does not optimize stomatal behaviour. *Plants*, 9, 1091.

Ricciuto, D., Sargsyan, K. & Thornton, P. (2018) The impact of parametric uncertainties on biogeochemistry in the E3SM land model. *Journal of Advances in Modeling Earth Systems*, 10, 297–319.

Rogers, A. (2014) The use and misuse of vc,max in earth system models. *Photosynthesis Research*, 119, 15–29.

Rogers, A., Medlyn, B.E., Dukes, J.S., Bonan, G., Caemmerer, S., Dietze, M.C. et al. (2017) A roadmap for improving the representation of photosynthesis in earth system models. *New Phytologist*, 213, 22–42.

Rüger, N., Condit, R., Dent, D.H., DeWalt, S.J., Hubbell, S.P., Lichstein, J.W. et al. (2020) Demographic trade-offs predict tropical forest dynamics. *Science*, 368, 165–168.

Schlesinger, W.H. & Jasechko, S. (2014) Transpiration in the global water cycle. *Agricultural and Forest Meteorology*, 189–190, 115–117.

Shugart, H.H. (1984) *A theory of forest dynamics: the ecological implications of forest succession models*. New York: Springer.

Slot, M., Nardwattanawong, T., Hernández, G.G., Bueno, A., Riederer, M. & Winter, K. (2021) Large differences in leaf cuticle conductance and its temperature response among 24 tropical tree species from across a rainfall gradient. *New Phytologist*, 232, 1618–1631.

Souza, D.C., Jardine, K.J., Rodrigues, J.V.F.C., Gimenez, B.O., Rogers, A. & McDowell, N. et al. (2021) Canopy position influences the degree of light suppression of leaf respiration in abundant tree genera in the Amazon forest. *Frontiers in Forests and Global Change*, 4, 723539.

Spanner, G.C., Gimenez, B.O., Wright, C.L., Menezes, V.S., Newman, B.D. & Collins, A.D. et al. (2022) Dry season transpiration and soil water dynamics in the central Amazon. *Frontiers in Plant Science*, 13, 825097.

Still, C.J., Page, G., Rastogi, B., Griffith, D.M., Aubrecht, D.M., Kim, Y. et al. (2022) No evidence of canopy-scale leaf thermoregulation to cool leaves below air temperature across a range of forest ecosystems. *Proceedings of the National Academy of Sciences*, 119, e2205682119.

Swaine, M.D. & Whitmore, T.C. (1988) On the definition of ecological species groups in tropical rain forests. *Vegetatio*, 75, 81–86.

Thornton, P.E. & Zimmermann, N.E. (2007) An improved canopy integration scheme for a land surface model with prognostic canopy structure. *Journal of Climate*, 20, 3902–3923.

Weerasinghe, L.K., Creek, D., Crous, K.Y., Xiang, S., Liddell, M.J., Turnbull, M.H. et al. (2014) Canopy position affects the relationships between leaf respiration and associated traits in a tropical rainforest in far north Queensland. *Tree Physiology*, 34, 564–584.

Wolf, A., Anderegg, W.R.L. & Pacala, S.W. (2016) Optimal stomatal behavior with competition for water and risk of hydraulic impairment. *Proceedings of the National Academy of Sciences*, 113, E7222–E7230.

Wolz, K.J., Wertin, T.M., Abordo, M., Wang, D. & Leakey, A.D.B. (2017) Diversity in stomatal function is integral to modelling plant carbon and water fluxes. *Nature Ecology & Evolution*, 1, 1292–1298.

Wright, I.J., Reich, P.B., Westoby, M., Ackerly, D.D., Baruch, Z., Bongers, F. et al. (2004) The worldwide leaf economics spectrum. *Nature*, 428, 821–827.

Wu, J., Serbin, S.P., Ely, K.S., Wolfe, B.T., Dickman, L.T., Grossiord, C. et al. (2020) The response of stomatal conductance to seasonal drought in tropical forests. *Global Change Biology*, 26, 823–839.

Zanne, A., Lopez-Gonzalez, G., Coomes, D., Ilic, J., Jansen, S., Lewis, S. et al. (2009) Data from: towards a worldwide wood economics spectrum. Dryad. *Dataset*.

Zanne, A.E., Westoby, M., Falster, D.S., Ackerly, D.D., Loarie, S.R., Arnold, S.E.J. et al. (2010) Angiosperm wood structure: global patterns in vessel anatomy and their relation to wood density and potential conductivity. *American Journal of Botany*, 97, 207–215.

Zhen, S., van Iersel, M.W. & Bugbee, B. (2022) Photosynthesis in sun and shade: the surprising importance of far-red photons. *New Phytologist*, 236, 538–546.

Zhou, S., Duursma, R.A., Medlyn, B.E., Kelly, J.W.G. & Prentice, I.C. (2013) How should we model plant responses to drought? an analysis of stomatal and non-stomatal responses to water stress. *Agricultural and Forest Meteorology*, 182–183, 204–214.

Ziegler, C., Dusenge, M.E., Nyirambangutse, B., Zibera, E., Wallin, G. & Uddling, J. (2020) Contrasting dependencies of photosynthetic capacity on leaf nitrogen in early- and late-successional tropical montane tree species. *Frontiers in Plant Science*, 11, 500479.

How to cite this article: Lamour, J., Souza, D.C., Gimenez, B.O., Higuchi, N., Chave, J., Chambers, J. et al. (2023) Wood-density has no effect on stomatal control of leaf-level water use efficiency in an Amazonian forest. *Plant, Cell & Environment*, 46, 3806–3821. https://doi.org/10.1111/pce.14704